MOTIONS OF A SAILING YACHT IN LARGE WAVES: AN OPENING SIMPLE INSTATIONARY MODELLING APPROACH

Fabio Fossati[1], **Sara Muggiasca**[2]

Abstract. *Due to the increasing demand of methods and tools for the analysis of yacht behaviour in a realistic environment and in particular the development of time domain approaches able to simulate yacht motion when under sail in a seaway, in recent years a number of Dynamic Velocity Prediction Programs have been developed. Up to now, while very interesting results are available regarding dynamic effects on hydrodynamic forces acting on the yacht hull and appendages, the physics of unsteady sail aerodynamics have received far less attention. In this paper an opening simple model is presented with the aim to reproduce unsteady sail aerodynamics taking into account three dimensional effects and unsteady mainsail-jib interaction. Under the assumption that certain time and length scales for the yacht and its wave pattern are short compared with the time and length scales of the wave motion, the yacht is modelled as a single point mass constrained to move on a surface governed by the equations of wave motion: normal and tangential equations of vessel motion are derived and solutions are investigated for an arbitrary two-dimensional wave motion.*

1 INTRODUCTION

One of the most challenging tasks in yacht design modelling and simulation is the development of methods and tools for the analysis of yacht behaviour in a realistic environment. One particularly difficult task is developing time domain approaches that simulate yacht motion, including manoeuvring and course-keeping, when under sail in a seaway. To overcome these difficulties, modelling must move from Velocity Prediction Programs (VPP) to Dynamic Velocity Prediction Programs.

In recent years a number of Dynamic Velocity Prediction Programs have been developed. To the authors' knowledge, the work of Spens, De Saix and Brown [1] is the first attempt to apply classical ship manoeuvring theory to sailboats. Several years later Letcher [2] proposed an analysis of off wind steering characteristics based on the classic root locus method for solving nonlinear differential equations. Professor Gerritsma [3] presented a paper in which the wave induced motions and manoeuvring characteristics of a typical offshore racing yacht have been analysed using a linear steering model with stability derivatives derived by Planar Motion Mechanism experiments. No treatment of rig influence was considered. In a following paper by Gerritsma and Moeyes [4] several hull forms and sails influence have been included in the phenomena analysis.

[1] Department of Mechanical Engineering - Politecnico di Milano - ORC ITC Research Associate
[2] Department of Mechanical Engineering, Politecnico di Milano

In 1995 Masuyama et al. [5] presented a model based on a force derivative approach: a very good correlation of numerical simulation with full scale results has been obtained by the authors using an experimental determination of the hydrodynamic coefficients. In particular coefficients describing the hull forces were determined by applying regression on the results obtained from dedicated experiments in the towing tank for the one particular yacht considered in his study. In the same paper a completely different approach has been also presented based on neural network schematization. The neural approach represents a very useful option even if does not provide any insight into the physics of the sail in unsteady flow.

One of the most generic model has been recently proposed by Keuning et al. [7]: this model is based on the idea of use the extensive results and database as obtained within the Delft Systematic Yacht Hull Series in order to generate generally applicable approximations for the coefficients in the equation of motions. The hydrodynamic model proposed by Keuning in [7] has been recently used by Battistin et al. ([8]) who developed a dynamic VPP, as a first feasibility study, as a plug-in of MSC ADAMS multi-body dynamics analysis tool.

After this literature survey and analysis we can conclude that while very interesting results are available regarding dynamic effects on hydrodynamic forces acting on the yacht hull and appendages, the physics of unsteady sail aerodynamics have received far less attention and are consequently less well understood.

Most of the abovementioned authors use the steady state approach based on force coefficients empirically derived or measured from wind tunnel experiments as a function of the apparent wind angle. As an example in [8] the aerodynamic forces are modelled following the IMS formulation ([9], [10]), i.e. a steady state approach, both for the lift and drag of sails and for windage elements. Some authors like in [7], [20], [21] and [22], include the induced velocities by the roll and the yaw motions into the apparent wind angle and apparent wind speed expressions following the so called Quasi Steady Theory (QST) approach. On the other side, in order to take into account unsteady effects also CFD simulations have been proposed: for instance Jacquin et al. [6] presented an “all inclusive” VPP-CFD simulations. These numerical methods include all the basic features of unsteady flow but they are still in an early development stage and are also computationally very expensive.

Very few experimental studies have recently addressed the unsteadiness of sails aerodynamics: in 2008 Gerhardt et al. ([11]) used unsteady potential flow theory to predict pressure distribution on a two dimensional “slice” of a mainsail carrying out harmonic oscillation both perpendicular to and along the direction of the incident flow and theoretical prediction has been compared to wind tunnel measurements on an oscillating 2D rigid mainsail slice model, leading to the conclusion that the aerodynamic performance can only be predicted using an aerodynamic unsteady model. The mainsail only analysis of Gerhardt et al. in ([12]) has subsequently been extended to a two sails configuration using a couple of 2D cambered profiles. The main finding however is still the same i.e. that the aerodynamics can be predicted more accurately with an unsteady model.

More recently Augier et al. ([18], [19]) presented a dedicated instrumentation system designed to perform full scale measurements of loads in standing and running rigging as well as yacht motion and in ([15], [26]) some results of pressure measurements at full scale are reported. In particular Augier’s papers are focused on the results obtained on an upwind port tack run in head moderate swell and underline the importance of an unsteady model to represent the flow and the stress in the sails in real condition.

To the authors’ knowledge, the only available experimental results specifically concerning unsteady sail aerodynamics were presented by the authors in [13], where unsteady aerodynamics has been investigated on a 3D sailplan by means of dynamic wind tunnel tests. Yacht induced pitch motion frequency and amplitude effects on sails forces have been

investigated by means of forced motion oscillation tests carried out by means of a rigid sailplan using a carbon fibre manufactured rig scale model of a 48' IMS cruiser-racer sloop: dynamic tests have been performed within the typical encounter frequency range and typical pitch amplitudes corresponding to best VMG condition for different true wind speed and relevant sea state highlighting some fundamental issues of the unsteady sail aerodynamics.

Preliminary obtained results have been used in [24] to address development of numerical models which could be easily incorporated into a Dynamic Performance Prediction Program for the analysis of sailing yacht behaviour in a realistic environment allowing for reproduce yacht sails aerodynamic coefficients in the time domain.

To extend the scope of the investigation further forced motion tests have been recently carried out on the same yacht rig equipped by traditional soft sails [27] in order to provide an insight into the sails flexibility effects on sails aerodynamics and a thorough investigation of the sailplan unsteady aerodynamics dependence on different yacht courses.

In the present paper the numerical approach outlined in [24] is embedded in a very simple time domain model which aims to simulate yacht motion when under sail in a seaway: this model should be considered just an opening model in an attempt to reproduce yacht pitch frequency and amplitude effects on sail aerodynamics taking into account three dimensional effects and unsteady mainsail-jib interaction.

The proposed model is based on the assumption that certain time and length scales for the yacht and its wave pattern are short compared with the time and length scales of the wave motion.

In particular the yacht is modelled as a single point mass constrained to move on a surface governed by the equations of wave motion: normal and tangential equations of vessel motion are derived and solutions are investigated for an arbitrary two-dimensional wave motion.

2 THE YACHT MODEL

The proposed mathematical model rely heavily on the assumption that the yacht dimensions are so small in comparison to the scale of the waves that her influence on the waves may be neglected and the time scale of her oscillations are short compared with the wave period.

Thus the vessel is modelled as a point mass which is constrained to move on the moving surface of the sea. The sea surface defined by the function $f(x,t)$ which represents an holonomic and rheonomous constraint and at any given time it is a general cylinder whose generators lie perpendicular to the true wind incoming direction (2D wave motion hypothesis of classical wave mechanics theory).

Curvature of the earth is neglected so gravity is a uniform parallel field of magnitude g_0.

The environment of the boat is shown in figure 1: the vessel runs straight on her course which forms a fixed angle μ between yacht centreline and true wind direction in a Cartesian frame with z axis vertical and x axis pointing along the yacht course.

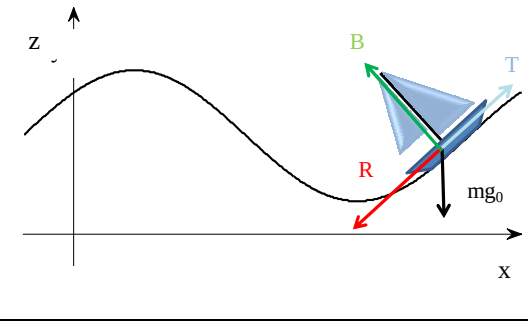

Yacht environment

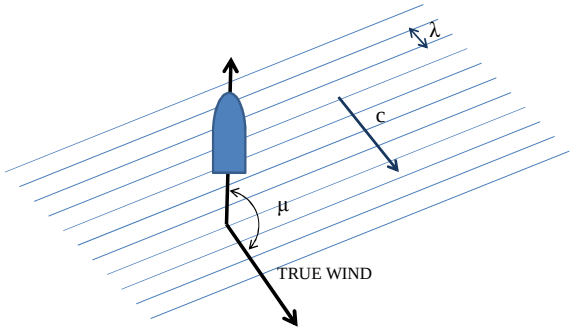

Yacht course vs wind and waves direction

Figure 1

The yacht is located by the coordinates:

$$\begin{cases} x = x(t) \\ z = f(x(t), t)) \end{cases} \tag{1}$$

The external wave motion is unaffected to first order by the presence of the vessel (due to the smallness of the yacht) and does not need to be specified at the moment: this can be described by means of any theory of two dimensional progressive waves including irregular sea environment.

2.1 KINEMATICS

Using eq.(1) to define the position of the yacht, differentiating we find the yacht's velocity V_B and acceleration A_B:

Position: $$\begin{cases} x = x(t) \\ z = f(x(t), t)) \end{cases} \tag{2}$$

Velocity: $$\begin{cases} V_X = \dfrac{dx(t)}{dt} = \dot{x}(t) \\ V_Z = \dfrac{df(x(t), t))}{dt} = f_x \dot{x} + f_t \end{cases} \tag{3}$$

Acceleration: $$\begin{cases} a_X = \dfrac{dV_X}{dt} = \ddot{x}(t) \\ a_Z = \dfrac{dV_Z}{dt} = f_x \ddot{x} + 2 f_{xt} \dot{x} + f_{xx} \dot{x}^2 + f_{tt} \end{cases} \tag{4}$$

where a dot means an ordinary derivative with respect to time and the subscripts x and t signify partial derivatives.

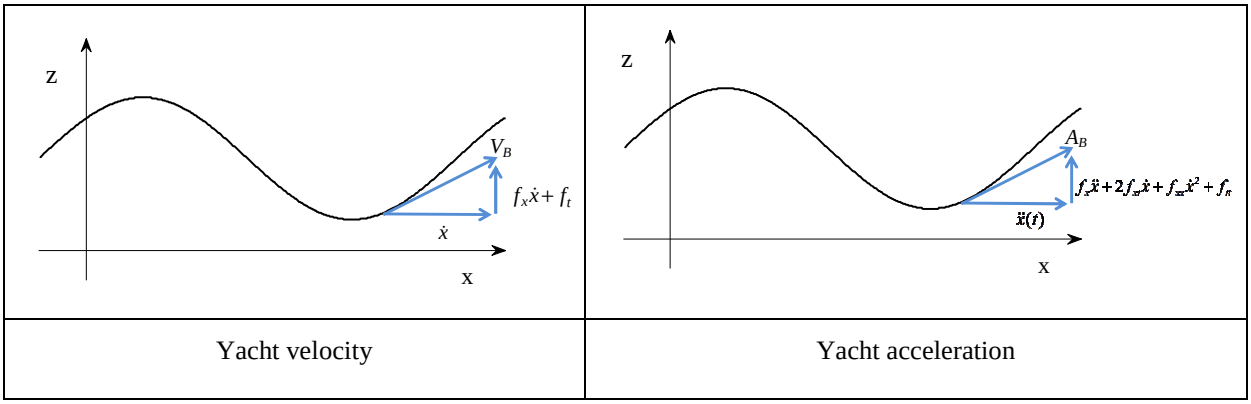

Yacht velocity	Yacht acceleration

Figure 2

The yacht's velocity and her acceleration can be resolved into normal and tangential components which are respectively defined by the following expressions (see Appendix 1):

$$V_n = f_t\left(1+f_x^2\right)^{-1/2} \tag{5}$$

$$V_t = \dot{x}\left(1+f_x^2\right)^{1/2} + f_x f_t\left(1+f_x^2\right)^{-1/2} \tag{6}$$

$$a_n = \left(f_{xx}\dot{x}^2 + 2f_{xt}\dot{x} + f_{tt}\right)\cos\sigma \tag{7}$$

$$a_t = \ddot{x}\left(1+f_x^2\right)^{1/2} + f_x a_n \tag{8}$$

2.2 DYNAMICS

The normal and tangential boat equation of motion can be considered according to the following expressions (fig.(3)):

$$ma_n = B - mg_0\cos\sigma \tag{9}$$

$$\tilde{m}a_t = T - R_{tot} - mg_0\sin\sigma \tag{10}$$

where:

B is the buoyancy (normal to the free surface)
T is the aerodynamic driving force (parallel to the surface)
R_{tot} is the total hydrodynamic resistance (parallel to the surface)
g_0 is the acceleration due to gravity (vertically downward)
$\sigma = tg^{-1}(f_x)$ is the free surface slope
m is the mass of the yacht
$\tilde{m}$ is the apparent mass for the longitudinal motion

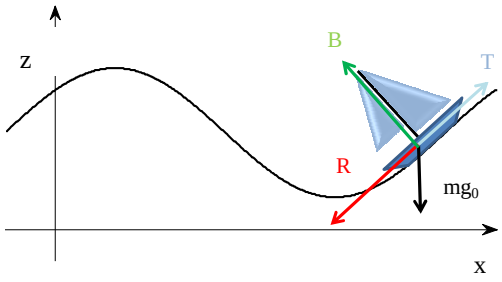

Figure 3

First consider the normal equation of motion: the yacht acceleration normal component is given in terms of x(t) by eq.(7) and buoyancy results from the normal pressure gradient acting on the surfaces of the yacht displaced volume ∇.

Defining with ρ_w water density and with $g(x,t)$ the normal acceleration on the free surface by Archimedes' principle buoyancy is given by:

$$B = \rho_w g(x,t)\nabla \tag{12}$$

It should also be noted that because of the wave motion the actual yacht displaced volume ∇ is different from the rest displacement ∇_0 which is related to the yacht mass by the following relationship:

$$m = \rho_w \nabla_0 \tag{13}$$

Thus, considering eq.(7) and eq.(13) the normal equation of motion becomes:

$$m\left(f_{xx}\dot{x}^2 + 2f_{xt}\dot{x} + f_{tt}\right)\cos\sigma = \rho_w g(x,t)\nabla - \rho_w \nabla_0 g_0 \cos\sigma \tag{14}$$

Because of the wave motion at some positions on the wave the vessel's normal acceleration is greater than that of the surrounding water and she displaces a larger volume that at rest while at some position the reverse will happen.

Let's consider now the tangential equation of motion: taking into account the yacht acceleration tangential component given by eq.(8) we have

$$\tilde{m}\left[\ddot{x}\left(1 + f_x^2\right)^{1/2} + f_x a_n\right] = T - R_{tot} - mg_0 \sin\sigma \tag{15}$$

In eq.(15) the mass is named $\tilde{m}$ to represent the longitudinal apparent mass of the yacht which includes the added mass. The apparent mass depends on the form of the hull, hence on the actual yacht displaced volume ∇.

For a typical streamlined form of a sailing yacht hull the added mass value is expected to fall in the range [2%-10%] of the yacht mass.

In conclusion eq. (15) is the general equation of motion which is a second order differential equation for the unknown position of the yacht $x = x(t)$ while eq.(14) can be used to evaluate the actual yacht displaced volume ∇.

As will be shown in the following, due to aero-hydrodynamics nonlinear characteristic numerical methods of forward integration must be used to find solutions from given initial conditions.

3 THE AERODYNAMIC MODEL

In order to evaluate aerodynamic thrust (figure 3) appearing in the yacht equation of motion (eq.15), the mathematical model proposed by the authors in [24] will be considered. This model rely on experimental data which can been obtained by means of dynamic wind tunnel tests and allows for reproduce yacht sails aerodynamic coefficients in the time domain.

Details of the experimental set-up and test methodology used in the dynamic wind tunnel tests can be found in ([13], [14]): for readers' convenience only a brief summary of the main points highlighted by experimental investigations will be provided in the following.

3.1 OUTLINE OF UNSTEADY SAIL AERODYNAMICS

Figure 4 shows the unsteady effects in sail aerodynamics due to the yacht pitch motions in waves. As can be seen both apparent wind speed V_{AW} and apparent wind angle β_{AW} corresponding to the steady state conditions change due to pitch induced velocity, resulting in a new apparent wind speed V_{ris} and a new apparent wind angle β_{din} which change in time and depend on the particular height considered.

Clearly the problem would be similar when we should take into account the effects of all the other motions not considered in the present paper.

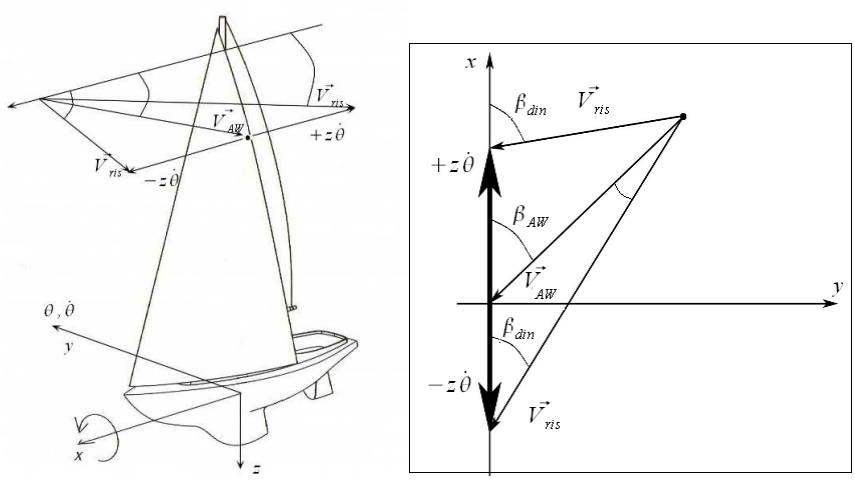

Figure 4: Dynamic effects on wind triangle

The starting point was to solve the wind triangle using the effective angle theory ([17]) on a plane perpendicular to the mast (figure 5) assuming the sailplan centre of effort as the reference point to define the instantaneous apparent wind speed and the instantaneous apparent wind angle.

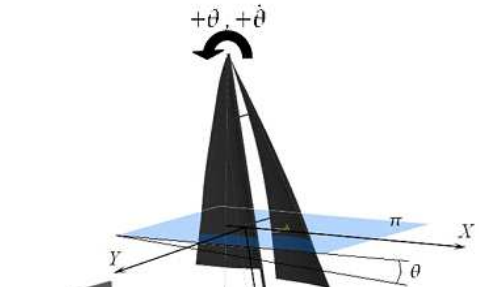

Figure 5: Reference plane π for the effective angle evaluation

When the yacht is pitched, the onset flow is no longer perpendicular to the leading edge of the sails and to account for this, the effective angle concept was used. The effective angle β_{eff} is geometrically related to the apparent wind angle β_{AW} as well as to the pitch angle θ and can be calculated from:

$$\beta_{eff} = tan^{-1}\left(\frac{tan\beta_{AW}}{\cos\vartheta}\right) \tag{16}$$

Similarly the effective wind speed V_{eff} can be obtained from β_{AW} and θ as a fraction of the apparent wind speed V_{AW} as follows:

$$V_{eff} = V_{AW}\sqrt{\left(\sin^2\beta_{AW} + \cos^2\beta_{AW}\cos\vartheta\right)} \tag{17}$$

The combination of the dynamic velocity at the centre of effort due to yacht pitch angular velocity with the steady-state effective speed V_{eff} leads to the dynamic wind speed V_{ris} and dynamic apparent wind angle β_{din} concepts as shown in Figure 6.

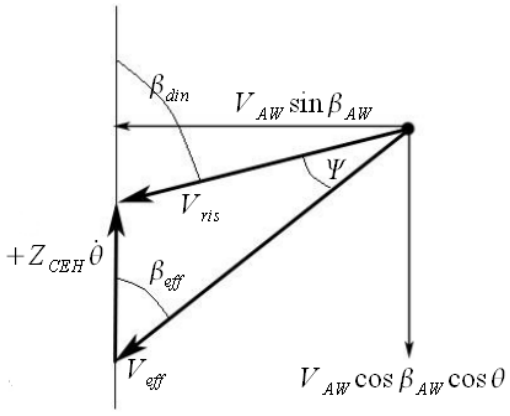

Figure 6: dynamic wind triangle

According to [14] a new representation of the aeroelastic effects is then proposed where aerodynamic forces are defined in dynamic conditions with reference to the dynamic wind triangle concept and are presented as a sort of aerodynamic hysteresis loops, obtained by

plotting the sailplan aerodynamic forces against the dynamic instantaneous apparent wind angle β_{din} evaluated at the instantaneous centre of effort height (Z_{CEH}) (figure 7).

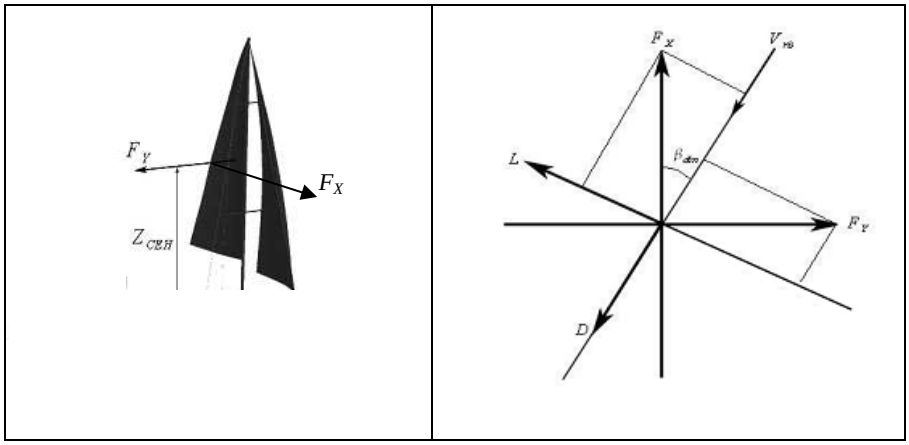

Figure 7: instantaneous centre of effort (left) and instantaneous aerodynamic forces (right)

In particular sail aerodynamic driving and heeling force coefficients (C_X and C_Y respectively) can be defined in the time domain as a function of the dynamic apparent wind angle β_{din} (i.e. the instantaneous angle of attack) according to the following relationship:

$$C_X = \frac{F_X}{\frac{1}{2}\rho V_{Ris}^2 S}$$
$$C_Y = \frac{F_Y}{\frac{1}{2}\rho V_{Ris}^2 S} \qquad (18)$$

where F_X and F_Y are respectively the measured aerodynamic driving and heeling forces components, S is the sailplan total area, ρ is the air density and V_{ris} is the dynamic resultant wind speed evaluated at the centre of effort height.

As an example, in figure 8 (taken from [13]) unsteady driving force coefficient C_X and heeling force coefficient C_Y obtained by means of pitch forced motion wind tunnel tests using a carbon fibre manufactured rig scale model of a 48' cruiser-racer sloop are plotted versus the dynamic apparent wind angle β_{din}. In the same figure dashed lines represent steady state aero-coeffs curves obtained by means of tests with the sails at rest.

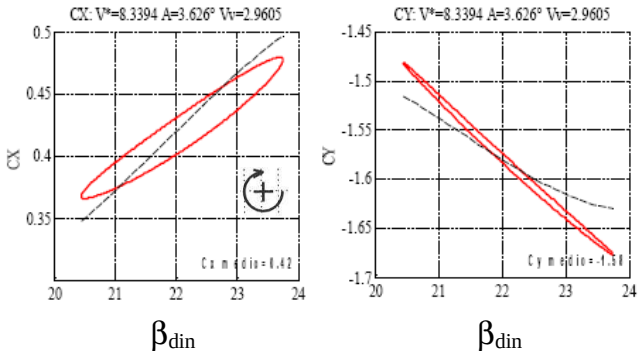

Figure 8 – Driving and heeling dynamic force coefficients vs. β_{din}

As can be seen the driving and heeling force coefficients developed in dynamic conditions are different for a given angle of incidence (dynamic apparent wind angle) depending on whether that angle is increasing or decreasing. This leads to an hysteresis loop, which denotes the presence of a phase shift between the force and the instantaneous angle of attack β_{din}. If the force and the instantaneous angle of attack were perfectly in phase, the hysteresis loop would appear as a single line equivalent to the static steady-state coefficient trend. When the force and the angle of attack are out of phase, the plot appears as a loop. In particular the direction of rotation of the loop indicates the relative phase between force and the instantaneous angle of attack and therefore the energy sign: clockwise (+ circles) indicates energy pumping, anticlockwise (- circles) indicates energy dissipation.

The area inside the loop represents the amount of energy that can be dissipated or put into the system by the aerodynamic forces depending on the sign of the phase shift. In our case the direction of rotation of the driving force coefficient loop is clockwise and this means that energy from the pitching motion (the waves) is converted into driving force (nevertheless this additional thrust force is of course at the cost of the damping force on the pitching yacht in waves).

The loop axis has a different slope with respect to the steady-state curve slope and this means that dynamic effects influence both the equivalent damping and stiffness characteristics of the aerodynamic forces field.

Another very important point concerning unsteady effects on sail aerodynamics highlighted by experimental investigations is the fundamental role of the reduced velocity V_R (or as an alternative the reduced frequency f_R). As well known, with reference to an oscillating airfoil, reduced velocity V_R (or as an alternative the reduced frequency f_R) are defined as follows:

$$V_R = \frac{V}{fC} = \frac{VT}{C}$$
$$f_R = \frac{fC}{V} = \frac{C}{VT} \qquad (19)$$

where:

- V is the flow velocity
- C is the airfoil chord
- f is the airfoil oscillation frequency
- T is the oscillation period (1/f)

Since the reduced frequency is directly proportional to the airfoil oscillation frequency, it is a parameter that expresses the speed with which the angle of incidence varies. It is also interesting to observe that the reduced velocity (eq.19) also expresses the relation between the airfoil oscillation period and the time (V/C) taken by a fluid particle to cover the length of the chord, or the time needed to cross the area interested by the wing section. Reduced frequency, which is the reciprocal of reduced velocity (as we can deduce from eq. 19) obviously expresses the converse relation. At this point it is easy to understand that, the shorter the time needed to cross the airfoil region is with respect to the time needed to complete an oscillation (the period T), that is for high values of reduced velocity or conversely for low values of reduced frequency, the more we can consider the conditions of the fluid-airfoil interactions to be static, and the more we can use the classic static or steady state formulation for calculating

the aerodynamic forces. On the other hand, the smaller the reduced velocity (or the greater the reduced frequency) the more the interaction conditions will differ from those of the static state and specific information on the forces developed in dynamic conditions would be needed.

Concerning the reduced frequency computation, moving from the airfoil to the sails situation, wind tunnel experiments showed that the sum of each sail chord measured in correspondence of the centre of effort height (Z_{CEH}) can be considered in order to provide the sailplan reference chord value (figure 9).

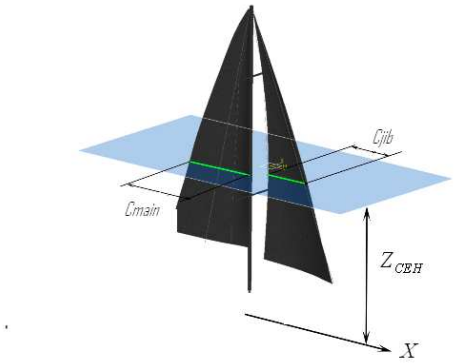

Figure 9: Sailplan chord length definition

As an example figures 10 (taken from [14]) show the driving and heeling force coefficients obtained by forced motion tests performed on the previous mentioned cruiser-racer sloop sailplan at 22° *AWA* with a pitch amplitude of 2° within the explored reduced velocity range (from V_R = 3 up to V_R = 42).

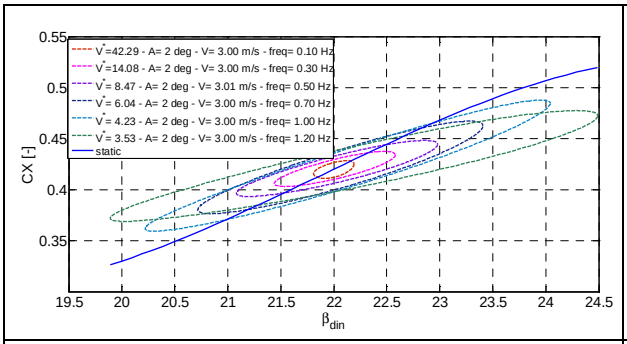

Driving force coefficient vs. β_{din} at different V_R

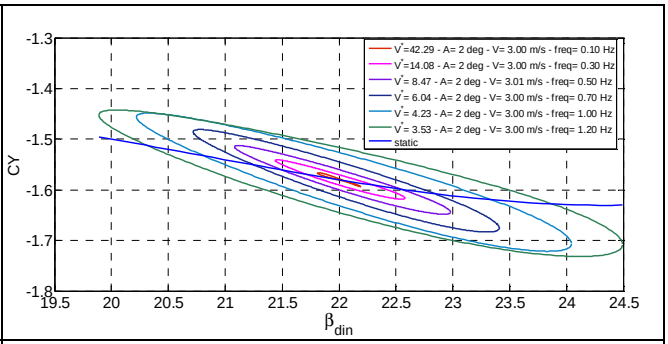

Heeling force coefficient vs. β_{din} at different V_R

Figure 10

A quite large amount of experimental tests recently carried out on both rigid and soft sails ([27]) confirm that reduced velocity play a fundamental role in sails aerodynamics and that yacht pitching motion has a strong and a non-trivial effect on the aerodynamic forces field. In particular as the reduced velocity decreases, the enclosed area of the hysteretic loop and the loop axis slope increase and this means that unsteady conditions lead to aerodynamic equivalent damping and stiffening effects.

3.2 SAIL AERODYNAMICS MODEL

As previously mentioned, in order to evaluate aerodynamic thrust (figure 3) appearing in the yacht equation of motion (eq.15), the mathematical model proposed by the authors in [24] will be considered. This model rely on experimental data obtained from dynamic wind tunnel tests and moves from the basic idea to compare the measured aerodynamic forces with the hysteretic effects measured on mechanical systems.

In fact it is possible to recognize that the hysteresis loop of the aerodynamic forces highlighted by experimental investigations and mentioned in the previous paragraph are similar to the typical hysteresis loop of a non-linear and non-conservative mechanical element leading to the possibility to develop a rheological model in the time domain in order to reproduce the sailplan aeroelastic forces based on the variation of the instantaneous apparent wind angle.

Generally speaking, rheological models, adopted to compute the aeroelastic forces induced by a variation in the instantaneous angle of attack, consist in a mechanical system whose components are springs, dampers, coulomb friction elements, bump stops and other mechanical parts that are interconnected and that react against the imposed motion (figure 11 left) and the modelled sails aerodynamic coefficient is given by the force transmitted to the ground by the equivalent mechanical system.

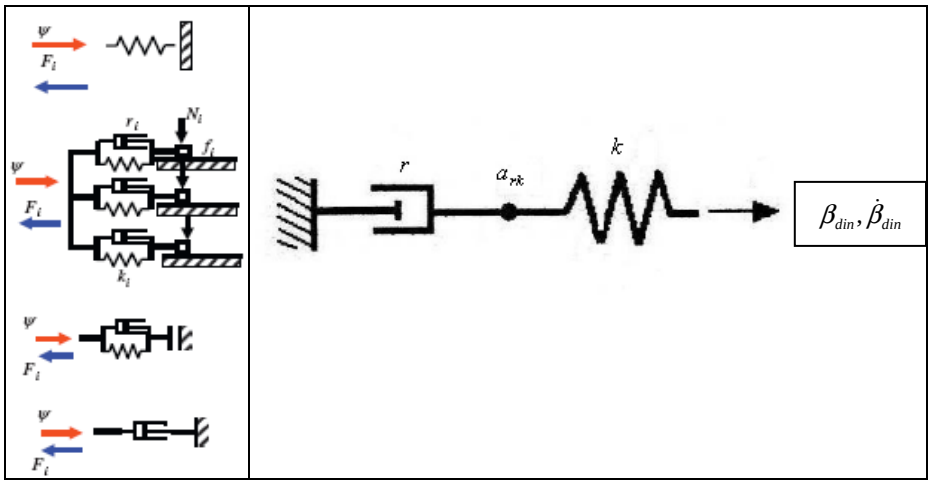

Figure 11: Typical rheological model components (left) and The proposed rheological model (right)

The input of the proposed model is the instantaneous apparent wind angle β_{din} and its time derivative $d\beta_{din}/dt$, being this angle function of the incoming nominal (steady state) apparent wind and of the yacht motion, in particular of the sailplan pitch angular velocity.

Moving on with the aerodynamics-mechanics analogy, the deformation of the mechanical system corresponds to the dynamic apparent wind angle in the sailplan, so that the mechanical force due to the imposed strains corresponds to the aerodynamic force due to a change in the instantaneous angle of attack on the sails. The major task, in the rheological model parameter identification, is to grant a good performance with the capability of reproduce both the reduced velocity dependence and the yacht motion amplitude dependence of the phenomenon.

Several models to compute the aeroelastic forces induced by a variation in the instantaneous angle of attack have been considered connecting different simple block like springs, dampers, coulomb friction elements, etc and, finally, the numerical model adopted consists in a mechanical system whose components are a linear spring with one extremity connected to a linear dampers as shown in figure 11 (right). Sail aerodynamic driving force

coefficient is equal to the force transmitted to the ground by the equivalent mechanical system resulting by the mutual interaction between the spring and the damper as a function of the instantaneous apparent wind angle β_{din} and its time derivative $\dot{\beta}_{din}$.

The dynamic behaviour of the proposed rheological system (fig.11 right) is described by the following equations:

$$\begin{cases} C_X = k(\beta - \alpha_{rk}) \\ r\dot{\alpha}_{rk} = k(\beta - \alpha_{rk}) \end{cases} \tag{20}$$

where the sailplan driving force coefficient C_X is assumed to be the force transmitted to the ground, which depends not only on the model input which is the instantaneous apparent wind angle β_{din} and its time derivative $\dot{\beta}_{din}$, but also on the spring-damper connecting point displacement α_{rk} and its time derivative $\dot{\alpha}_{rk}$ which can be obtained considering the following incremental relationship:

$$\alpha_{rk}(t+dt) = \alpha_{rk}(t) + \frac{dt}{r} * k\left(\beta(t) - \alpha_{rk}(t)\right) \tag{21}$$

Tuning properly the spring stiffness parameter k and damper damping parameter r allows for taking into account the aerodynamic equivalent damping and stiffness variation with the reduced velocity.

For the present work rheological model parameters have been identified, within a suitable range of reduced velocities, using experimental data provided by a quite large amount of dynamic wind tunnel tests carried out at 22°-27°-32° apparent wind angles in order to comply with the typical upwind sailing conditions [27].

As an example figure (12) summarizes driving force coefficients obtained within the explored reduced velocity range with a model pitch amplitude of 2°. As can be seen, aerodynamic thrust developed in dynamic conditions denotes the presence of a phase shift between the force and the instantaneous angle of attack β_{din} leading to groups of hysteresis loops placed in correspondence of each mean apparent wind angle within the considered range.

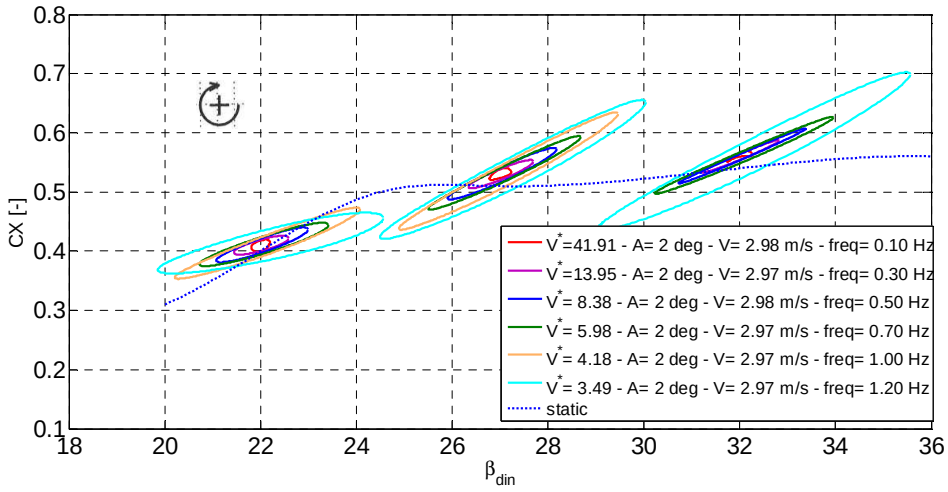

Figure 12

Using these results the rheological model parameters may be identified using a weighted least square curve fitting algorithm that minimizes the error between the experimentally measured hysteresis loops and those produced by the numerical model. Following this approach, for each of the investigated apparent wind angle, rheological model parameters dependence on reduced velocity can be assessed and reproduced by means of piecewise-linear fitting functions.

Figure 13 shows the stiffness and damping parameters trend vs the reduced velocity, which have been identified using experimental results reported in fig. 12.

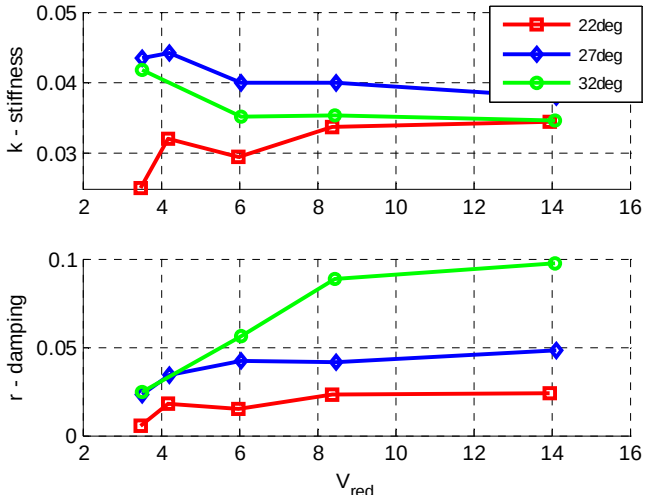

Figure 13: Driving force coefficient-rheological model parameters vs. reduced velocity

Let's consider now again the vessel running straight on her course and moving on the sea surface in a plane which forms a fixed angle μ between yacht centreline and the incoming waves: assuming the atmospheric wind blowing with speed W in the same direction of the waves and defining the true wind angle β_{TW}, we can consider the tangential component using the surface angle σ which will define the true wind speed W_{TW} in the π plane perpendicular to the mast (figure 14):

$$V_{TW} = W\cos\sigma = \frac{W}{\sqrt{\left(1+f_x^{\,2}\right)}} \qquad (22)$$

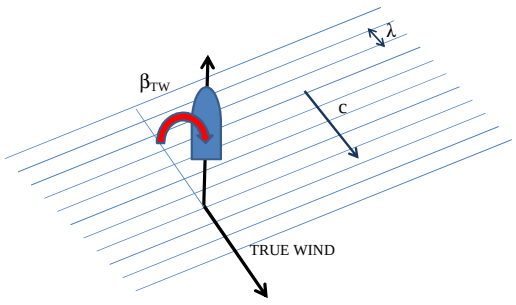

Yacht course vs true wind and waves direction

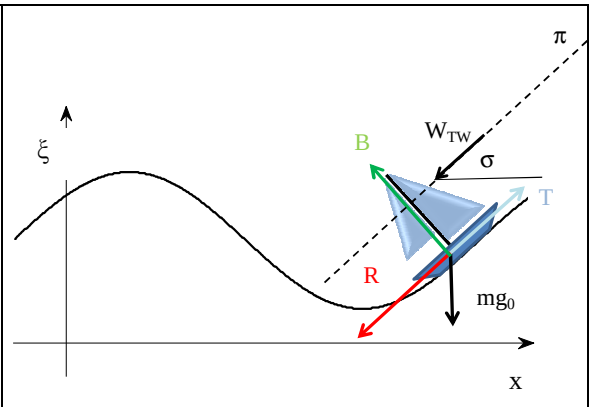

Effective angle theory plane

Figure 14

According to effective angle theory, taking into account for the yacht's velocity tangential component we can define the dynamic resultant wind speed V_{ris} and the dynamic instantaneous apparent wind angle β_{din} in the π plane using the following equations:

$$V_{ris}^2 = (V_t + W_{TW}\cos\beta_{TW})^2 + (W_{TW}\sin\beta_{TW})^2$$
$$\beta_{din} = arctg\left(\frac{W_{TW}\sin\beta_{TW}}{V_t + W_{TW}\cos\beta_{TW}}\right) \tag{23}$$

Finally the aerodynamic thrust (figure 14) appearing in the yacht equation of motion (eq.15) can be evaluated by means of the following expression:

$$T = \frac{1}{2}\rho_a S\, C_X(\beta_{din}) V_{ris}^2 \tag{24}$$

where S is the sailplan total area, ρ_a is the air density and C_X is the unsteady aerodynamic driving force coefficient which can be evaluated at each time step by means of equations (20) using the stiffness and damping parameters chosen in correspondence of the reduced velocity obtained combining the relevant wave frequency and wind speed values.

4 THE HYDRODYNAMIC MODEL

As far as the total hydrodynamic resistance R_{tot} which appears in the yacht equation of motion (eq.15) is concerned, in the present paper the choice was to include a formulation which would be as much simpler as possible but able to include the effects due to the actual yacht displaced volume ∇ variation under the effective gravitational acceleration $g(x,t)$.

As usual the total hydrodynamic resistance has been split into frictional and wavemaking components as summarized in the following.

Under the model assumptions highlighted in par. 2 and taking into account the tangential velocity V_{H2O} of a water particle on the free surface, the hull is travelling at a speed:

$$V_t - V_{H2O} \tag{25}$$

at a displacement ∇ in locally flat water, under the effective gravitational acceleration $g(x,t)$. Considering:

the Reynolds number:

$$\mathrm{Re} = \frac{(V_t - V_{H2O})LWL}{\upsilon} \tag{26}$$

the Froude number:

$$Fn = \frac{(V_t - V_{H2O})}{\sqrt{g(x,t)LWL}} \tag{27}$$

and assuming these dimensionless quantities with the actual yacht displaced volume ∇ are the parameters describing the current geometry and flow conditions, the frictional resistance component is evaluated according to the following expression:

$$R_f = \frac{1}{2}\rho_w A_w(\nabla)\,(V_t - V_{H2O})^2 C_{Rf} \tag{28}$$

where:

R_f is the frictional resistance
ρ_w is the water density
A_w is the hull wetted surface
C_{rf} is the skin friction coefficient

The skin friction coefficient has been evaluated using the well-known ITTC 57 formula.

The wavemaking resistance component has been evaluated according to the MIT-VPP original formulation [25]:

$$R_w = \frac{1}{10^5}\rho_w g \nabla a_1 \left(\frac{BWL}{Tc}\right)^{a_2} \frac{C_v}{\sqrt{C_v^2 + a_3}} \tag{29}$$

where:

R_W is the wavemaking resistance component
Tc is the canoe body draft
BWL is the theoretical waterline beam
C_v is the volumetric coefficient
∇ is the actual canoe body displaced volume
g is the acceleration of gravity
ρ_w is the water density

The values of the coefficients a_1, a_2 and a_3 are a function of the relative speed $\sqrt{\frac{V_t}{LWL}}$ and are reported in [25]

5 SOLUTION OF EQUATIONS OF MOTION

In order to find solutions of the normal and tangential equations of motion of the vessel moving on the free surface due to nonlinearities of aero-hydrodynamic force fields, numerical methods of forward integration must be used from given initial conditions.

As a consequence of nonlinear formulations of the aerodynamic thrust and of the total hydrodynamic resistance outlined in the previous paragraphs, the general equation of motion (eq. (15)) is a nonlinear second order differential equation for the unknown position of the yacht $x = x(t)$: this equation has been solved using a modified Newmark method including a frozen time iterations loop at each time.

More in details, due to the dependence of both frictional and wavemaking resistance components on the actual displaced volume ∇ moving from step *n* to *n+1*, the yacht position velocity and acceleration are evaluated using a frozen time iteration loop where, at each iteration, eq.(14) is used to calculate the yacht displaced volume ∇ requested to evaluate the abovementioned force components.

6 SOME RESULTS

The proposed mathematical model has been used to investigate the dynamic response of a 48' cruiser-racer sloop whose main dimensions are shown in table 1.

LOA (m)	14.5
BMAX (m)	4.29
LWL (m)	13.05
BWL (m)	3.78
DISPL (kg)	14300
SAIL AREA (m^2)	114
AW (m^2)	45.5
Tc (m)	0.83

Table 1. Main yacht dimensions.

6.1 REGULAR WAVES

Analyses have been initially carried out considering yacht sailing in regular waves and equations (14) and (15) have been specialized taking into account linear wave theory formulation.

In particular the surface profile is described by the following equation:

$$\xi(x(t),t)) = \xi_0 \cos(kx + \omega_e t) \tag{30}$$

where

ξ_0 is the wave amplitude
k is the wave number
ω_e is the encounter frequency

The encounter frequency is evaluated by means of:

$$\omega_e = \omega - k\dot{x}\cos\mu \tag{31}$$

where $\dot{x}$ is the yacht speed and μ is the heading angle (fig.1).

The incoming wave direction is assumed to be the same as the direction of the true wind, so the true wind angle *TWA* can be related to the heading angle of equation (15) according to:

$$TWA = 180° - \mu \tag{32}$$

True wind speed and true wind angle values were chosen in such a way to match apparent wind angle values where aerodynamic thrust coefficient hysteresis loops are available from dynamic wind tunnel tests.

In particular steady state analyses have been performed at the beginning, considering only the longitudinal steady equations of motion:

$$T - R_{tot} = 0 \tag{33}$$

with reference to the following cases (table2):

CASE	TWA (deg)	TWS (knots)
#1	44.7	6
#2	38.8	20
#3	60	10

Table 2

leading to steady state yacht speed and apparent wind angle values reported in table 3.

CASE	Yacht speed (knots)	AWA (deg)
#1	6.6	22
#2	9.4	26.5
#3	7.8	32.1

Table 3

Then regular waves have been considered and, in order to link wind intensity to significant wave height and period properties, relationships relating to the North Atlantic [28] were used (Figure 15).

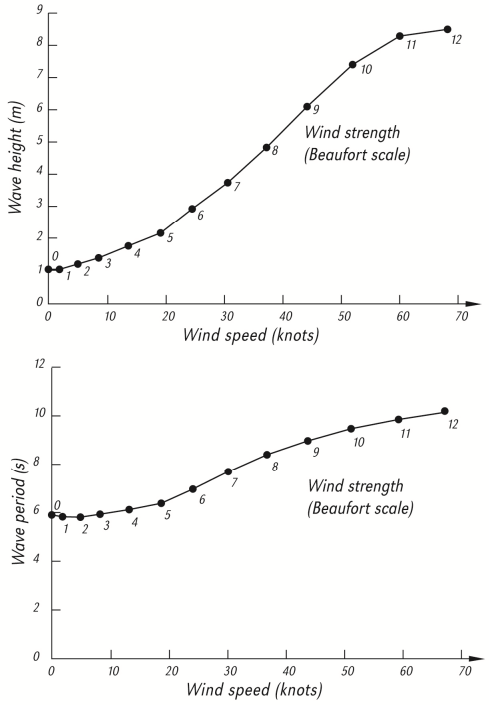

Figure 15. Wave significant height and wave period versus wind speed.

More in details table 4 shows the wave height and period values considered for analyses carried out on yacht sailing in regular waves.

CASE	TWS (knots)	Hs (m)	T0 (s)
#1	6	1.2	5.8
#2	20	2.2	6.8
#3	10	1.5	6

Table 4. Wave height and wave period values

In the following, results obtained with reference to CASE #1 are shown.

In particular fig. 16 shows the regular wave surface encountered by the yacht sailing under her way and figures 17 and 18 show respectively the tangential component of the yacht speed and the actual displaced volume time histories. Starting from initial conditions which correspond to steady state solution obtained as previously described, the yacht velocity develops as dynamic oscillations with encounter period of 4.56 [s] which results out of phase with the wave profile, as well as the actual volume displacement. Little by little time is increasing yacht speed oscillations becomes stationary in the neighbourhood of a mean value which is about 95% of the steady state problem solution (eq.33).

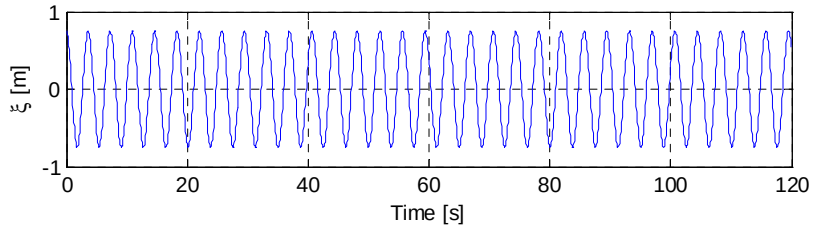

Fig. 16: CASE #1- wave profile time history

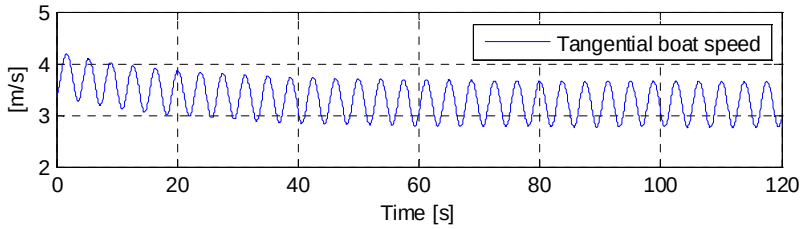

Fig. 17: CASE #1- tangential yacht speed time history

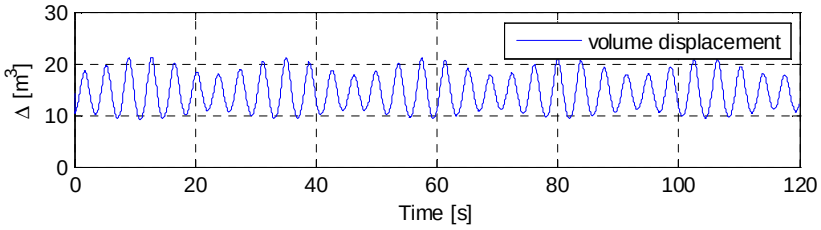

Fig. 18: CASE #1- actual displaced volume time history

Figures 19-20 show the dynamic apparent wind angle and speed time histories, due to the wave induced pitch oscillation which have been used to evaluate the dynamic aerodynamic driving force coefficient (fig. 21). In particular at each time step the aerodynamic driving force coefficient has been obtained by means of numerical integration of the rheological model equations (20); stiffness and damping parameters appearing in eq.(20) have been selected from red curves of figure 13 in correspondence of the reduced velocity value resulting from the considered mean apparent wind speed and encounter frequency.

Figure 20 shows the comparison between the driving force coefficient hysteretic loop obtained by the numerical model and the experimental one.

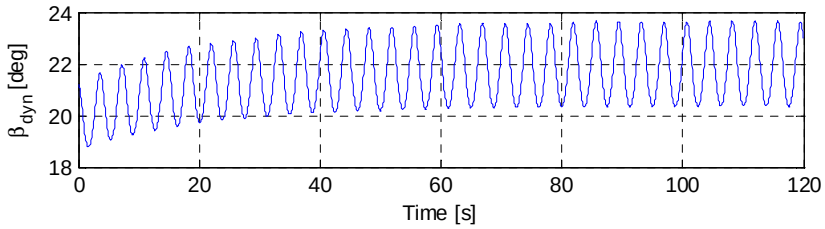

Fig. 19: CASE #1- dynamic apparent wind angle time history

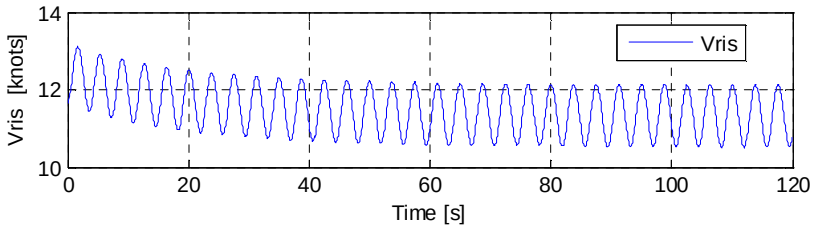

Fig. 20: CASE #1- dynamic apparent wind speed time history

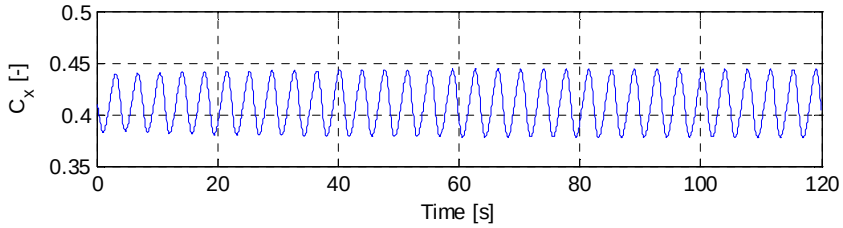

Fig. 21: CASE #1- dynamic aero-coefficient time history

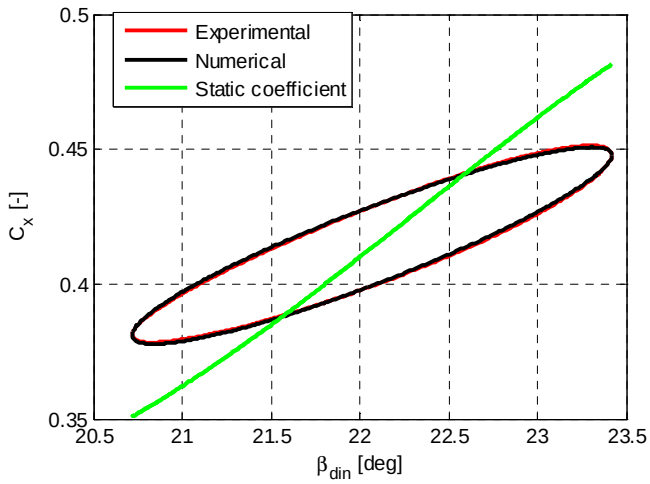

Fig. 22: CASE #1- aerodynamic driving force coefficient

Finally figure 23 shows the hydrodynamic total resistance and aerodynamic force time histories.

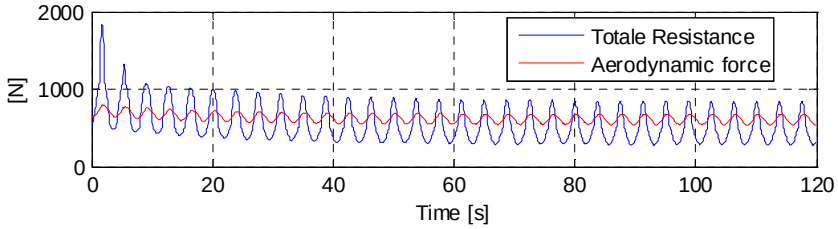

Fig. 23: CASE #1- total hydrodynamic resistance and aerodynamic thrust time histories

In the following the same results obtained for CASE#2 are reported.

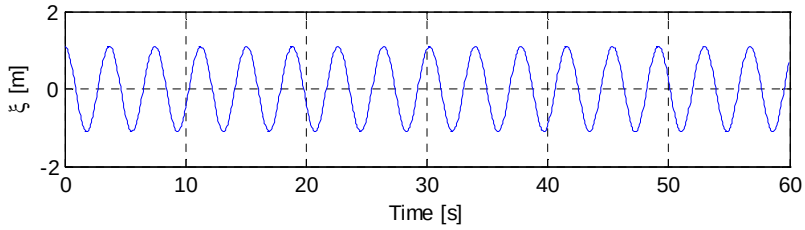

Fig. 24: CASE #2- wave profile time history

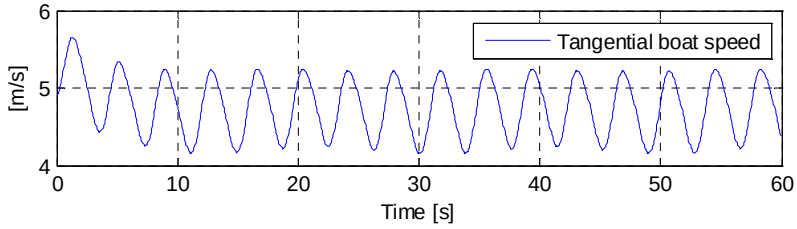

Fig. 25: CASE #2- tangential yacht speed time history

In this case yacht speed oscillations becomes stationary in the neighbourhood of a mean value which is about 3% less of the steady state problem solution.

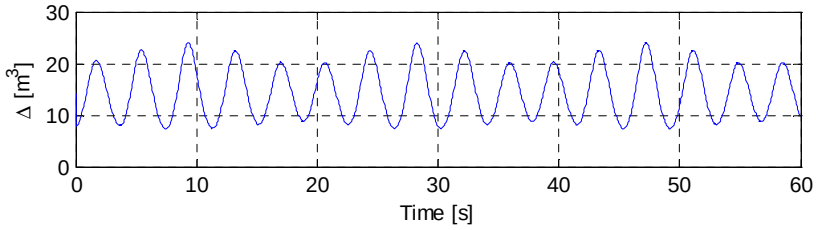

Fig. 26: CASE #2- actual displaced volume time history

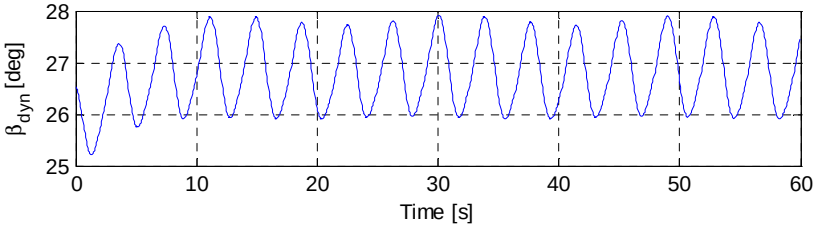

Fig. 27: CASE #2- dynamic apparent wind angle time history

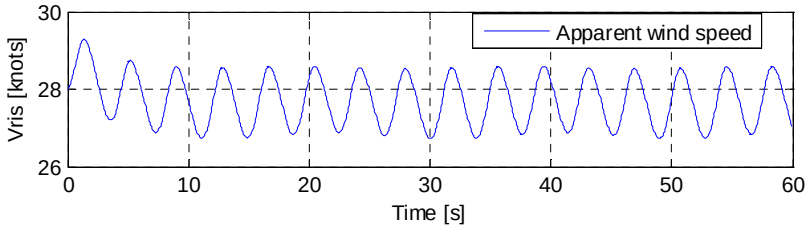

Fig. 28: CASE #2- dynamic apparent wind speed time history

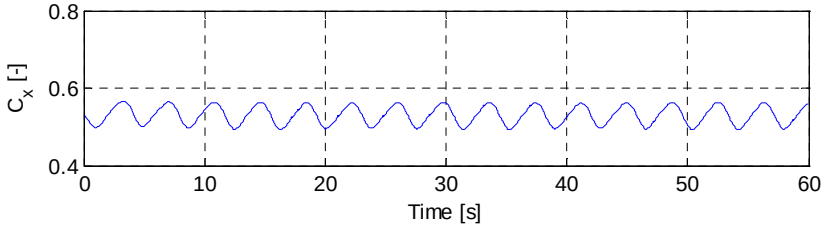

Fig. 29: CASE #2- dynamic aero-coefficient time history

Finally results of CASE#3 are reported in the following.

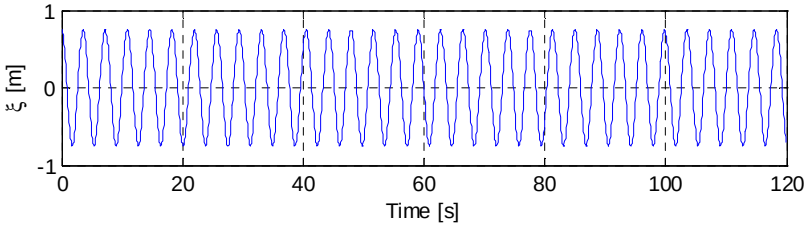

Fig. 30: CASE #3- wave profile time history

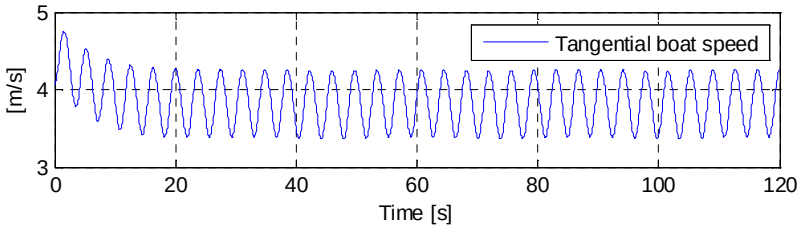

Fig. 31: CASE #3- tangential yacht speed time history tory

In this case yacht speed oscillations becomes stationary in the neighbourhood of a mean value which is about 5-6% less of the steady state problem solution.

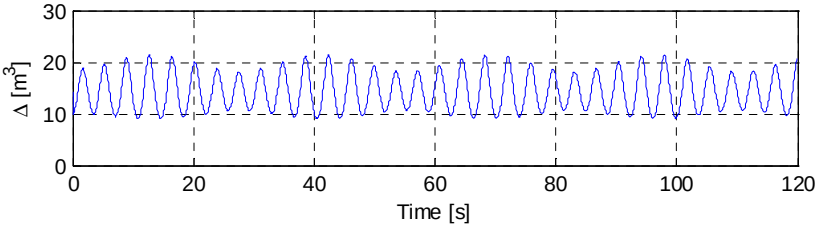

Fig. 32: CASE #3- actual displaced volume time history

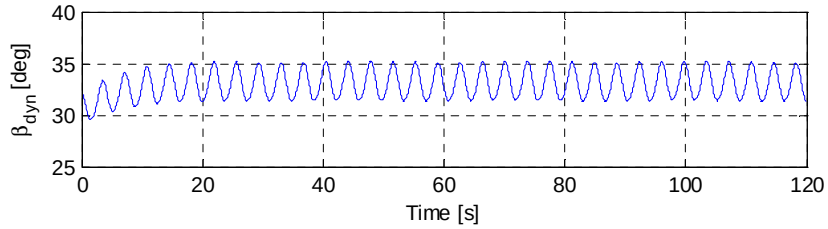

Fig. 33: CASE #3- dynamic apparent wind angle time history

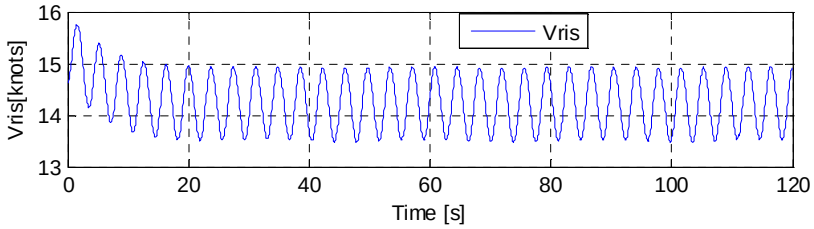

Fig. 34: CASE #3- dynamic apparent wind speed time history

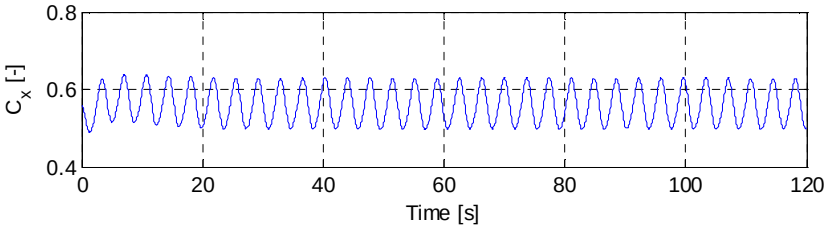

Fig. 35: CASE #3- dynamic aero-coefficient time history

As a general comment even if the obtained results could be certainly, to a certain extent, considered overall unrealistic in terms of yacht speed and displaced volume due to the model simplicity, on the other side it can be said that the proposed model, which moves from basic principle of hydrodynamics and mechanics, is leading to a description of yacht motions in waves that agrees qualitatively with many aspects of the real life situation.

6.1 IRREGULAR WAVES

The proposed model has been also used to investigate the yacht behavior in irregular sea.

Realistic irregular waves have been obtained using an idealised wave energy spectrum: several formulas exist for expressing in analytical form the idealized wave energy spectra as a function of characteristic parameters such as the significant wave height ($H_{1/3}$) and the average period (T_0) of the spectrum and for the present study the Bretschneider energy spectrum, which is particularly suited for representing conditions in mid ocean, was used.

Waves time histories have been synthesized by adding a large number of component sine waves according to the following expression:

$$\xi(x(t),t)) = \sum_{n=1}^{\infty} \xi_{n0} \cos\left(k_n x + \omega_{en} t + \phi_n\right) \tag{34}$$

where phase angles ϕ_n are chosen from a random distribution.

Again wave sea spectrum significant wave height and modal period are linked to the true wind speed using relationships reported in figure 15.

Analyses have been carried out considering the same true wind speed and true wind angles used in the previously shown regular waves cases (tab. 2) and for each case relevant wave height and period (reported in table 4) have been assumed as significant wave height and modal period values defining the Bretschneider energy spectrum.

The maximum frequency considered in the eq. (34) has been limited in such a way that the presence of irregular wave motion could not affect substantially the dynamic response of the yacht.

At this aim the yacht pitch amplitude and frequency range caused by the waves passing beneath it were estimated using the main yacht dimensions (Table 1) and the heave and pitch Response Amplitude Operator (RAO) for Model 455 from the DSYHS, obtained from towing tank tests and kindly provided by Prof. Keuning of Delft University of Technology.

This model has similar characteristics to the yacht here under analysis and figure 36 (left) shows the abovementioned pitch/wave slope RAO as a function of the LWL/wavelength ratio.

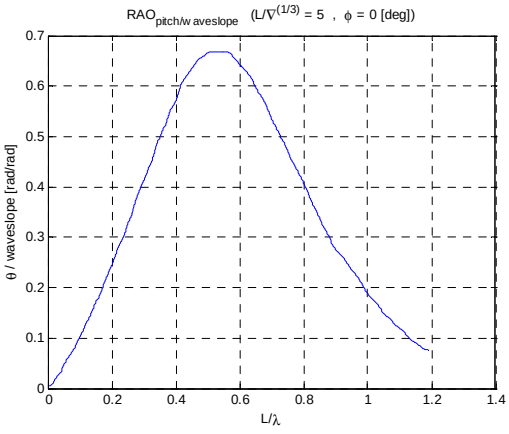

Pitch Response Amplitude Operator vs. L_{WL}/λ.

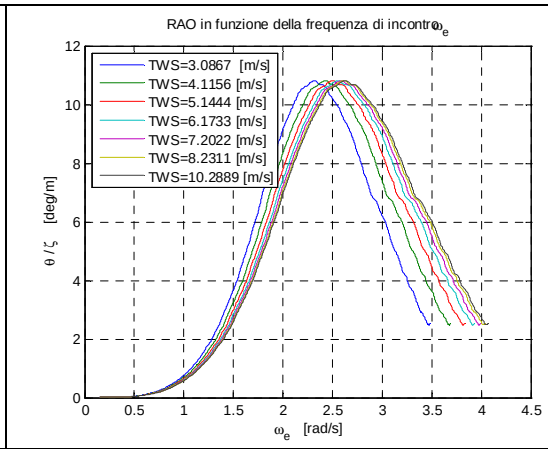

Pitch Response Amplitude Operator vs. encounter frequency

Figure 36

In order to estimate the yacht encounter frequency range, performance predictions at different true wind speeds and true wind angles were obtained using the longitudinal steady equations of motion (eq.33). The yacht VMG and the corresponding apparent wind angle were evaluated for each TWS (within the 6-20 [knots] TWS range). Then the corresponding yacht encounter frequency ranges were calculated using the abovementioned values and fig. 36 (right) shows the obtained pitch RAOs as a function of the encounter frequency.

The final step is to evaluate the pitch response in waves. At this aim the abovementioned Bretschneider energy spectra have been considered for the same true wind intensities (fig.37 left) and finally the pitch response spectra have been calculated by the product of the square of the motion RAOs and the wave energy spectra at the various wind intensities (fig.37 right) showing that the yacht pitch response spectra is defined within the range (1-4 [rad/s]).

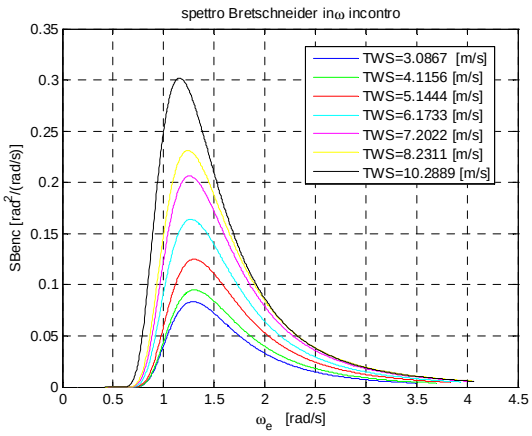

Yacht course vs wind and waves direction

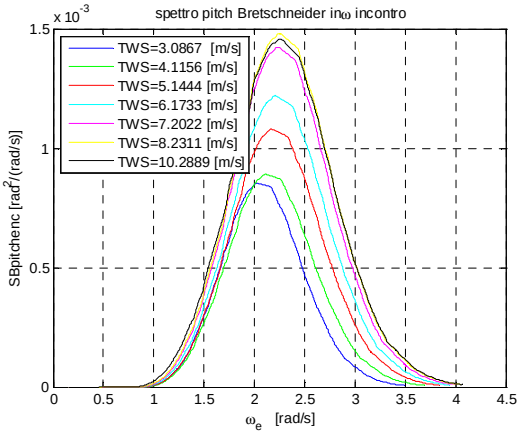

Yacht environment

Figure 37

As an example, results reported in the following refer to a seastate synthetized with the reference values reported in Tab.5 and fig. 38 shows the relevant energy spectrum.

TWA (deg)	TWS (knots)	Hs (m)	T0 (s)
60	10	1.5	6

Table 5. wind characteristics and irregular sea significant wave height and modal period

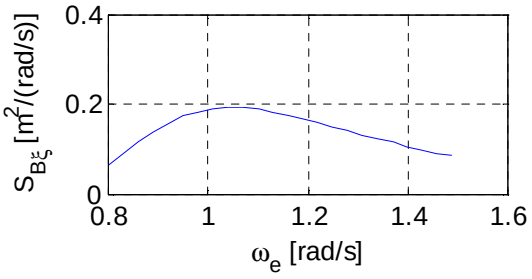

Fig. 38

Comparing fig. 37 right with figure 38 it can be seen that frequency yacht pitch response spectrum and wave energy spectrum have a very weak overlapping according to the maximum frequency chosen to define irregular wave time history in order to comply with the model basic assumptions.

Fig. 40 shows the irregular wave surface encountered by the yacht and figures 41 and 42 show respectively the tangential component of the yacht speed and of the actual displaced volume time histories.

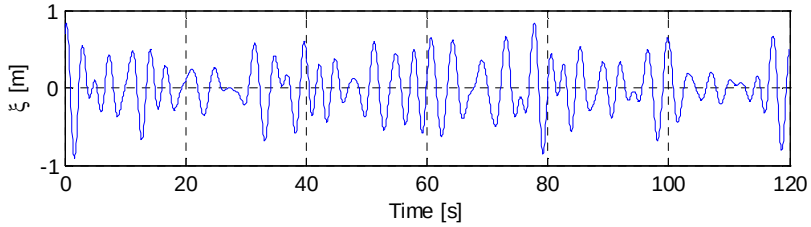

Fig. 40: irregular wave profile time history

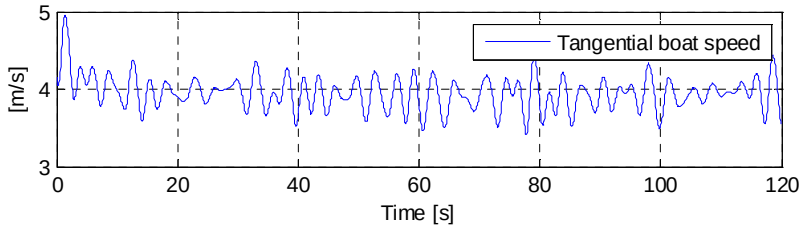

Fig. 41: irregular wave - tangential yacht speed time history

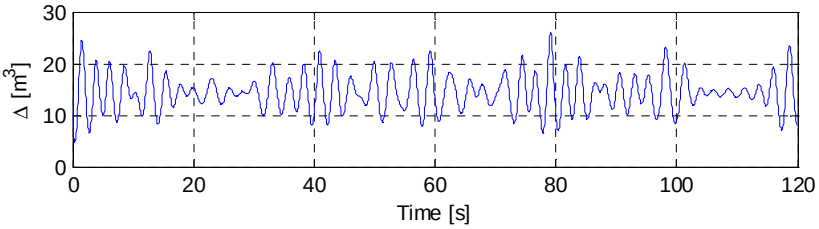

Fig. 42: irregular wave - actual displaced volume time history

Figures 43-44 show the dynamic apparent wind angle and speed time histories, due to the wave induced pitch oscillation which have been used to evaluate the dynamic aerodynamic driving force coefficient (fig. 45).

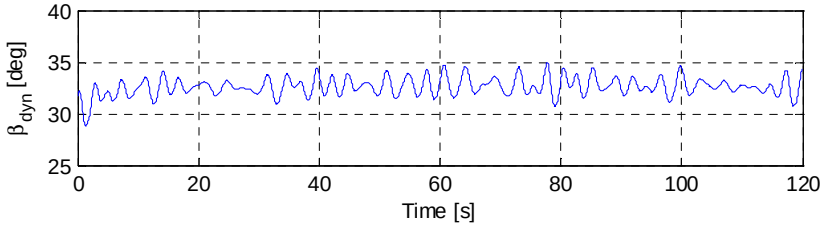

Fig. 43: irregular wave - dynamic apparent wind angle time history

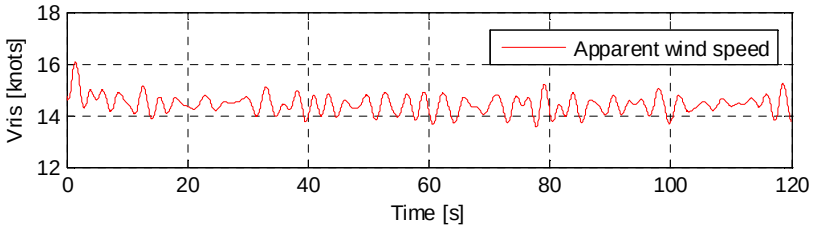

Fig. 44: irregular wave - dynamic apparent wind speed time history

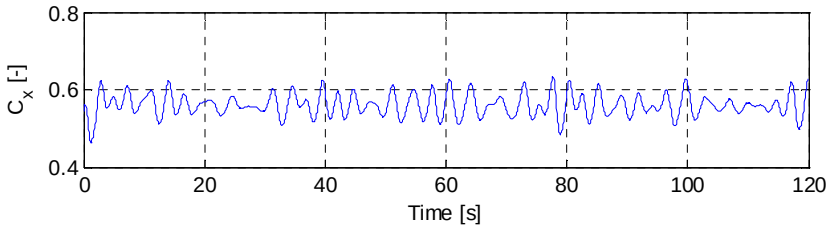

Fig. 45: irregular wave - dynamic aero-coefficient time history

In this case, in order to select the rheological model parameters values, a reference reduced velocity value has been considered based on the steady state apparent wind speed and on the modal encounter frequency appearing in the wave spectrum (fig. 38).

7 CONCLUSIONS AND FUTURE DEVELOPMENTS

This paper describes a very simple time domain model which aims to simulate yacht motion when under sail in a seaway. The proposed approach should be considered just a first step of a more comprehensive general research with the final goal to develop methods and tools for the time domain analysis of yacht behaviour in a realistic environment.

At present well-established results are available on dynamic effects on hydrodynamic forces acting on the yacht hull and appendages, while the physics of unsteady sail aerodynamics have received far less attention and are consequently less well understood.

In the present paper unsteady sail aerodynamics is embedded in a very simple time domain model which aims to simulate yacht motion in a seaway: in particular the yacht is modelled as a single point mass constrained to move on a surface governed by the equations of wave motion and sail aerodynamics is introduced moving from the idea to compute sail aeroelastic forces induced by a variation in the instantaneous angle of attack by means of rheological models able to represent hysteretic effects of unsteady sail aerodynamics highlighted by experimental results obtained from dynamic wind tunnel tests.

The proposed model is strongly relying on the assumption that certain time and length scales for the yacht and its wave pattern are short compared with the time and length scales of the wave motion and represents just a first attempt to reproduce yacht induced pitch motion effects on sail aerodynamics taking into account three dimensional effects and unsteady mainsail-jib interaction.

Author's view is that the proposed model, which moves from basic principle of hydrodynamics and mechanics could be improved in order to include some important additional features leading to a more realistic description of yacht motions in waves; in particular sail aerodynamics dependence on pitch motion amplitude and frequency could be included in the proposed aero-model, as well as a more realistic description of the yacht time scales oscillations including added mass and damping effects due to pitch, heave and surge motions. Finally an added resistance in waves formulation could be included in order to allow the designer to make comparison between various sailing yacht designs in the actual environmental conditions.

REFERENCES

[1] Spens P.G., DeSaix P., Brown P.W., 'Experimental studies of the sailing yacht', SNAME Transaction, 1967.

[2] Letcher, J.S., 'Steering qualities off the wind', *AIAA Symposium on the Aero-Hydronautics of Sailing*, AIAA, 1971.

[3] Gerritsma J.: 'Course keeping qualities and motions in waves of a sailing yacht' - *Technical Report, Delft University of Technology*, May, 1971.

[4] Gerritsma J., Moyes G., 'The seakeeping performance and steering properties of Sailing Yachts', *3rd HISWA Symposium on Yacht Design and Construction,* Amsterdam 1973.

[5] Masuyama Y., Fukasawa T., Sasagawa H., 'Tacking simulation of a sailing yacht - Numerical integration of equations of motion and application of neural network technique', *Proceedings of the 12th Chesapeake Sailing Yacht Symposium*, Annapolis, 1995.

[6] Jacquin E., Roux Y., Guillerm P.E., Alessandrini B., 'Toward numerical VPP with the full coupling of hydrodynamic and aerodynamic solvers for ACC yacht', *Proceedings of the 17th Chesapeake Sailing Yacht Symposium*, Annapolis, 2005.

[7] Keuning J.A., Vermeulen K.J., de Ridder E.J., 'A generic mathematical model for the maneuvering and tacking of a sailing yacht', *Proceedings of the 17th Chesapeake Sailing Yacht Symposium*, Annapolis, 2005.

[8] Battistin D., Ledri M., 'A Tool for Time Dependent Performance Prediction and Optimization of Sailing Yachts', *Proceedings of the 18th Chesapeake Sailing Yacht Symposium*, Annapolis, 2007.

[9] Claughton, A., 'Developments in the IMS VPP formulations', *Proceedings of the 14th Chesapeake Sailing Yacht Symposium*, Annapolis, 1999.

[10] Fossati F., Claughton A., Muggiasca S., Battistin D.,: 'Changes and Development to Sail Aerodynamics in the ORC International Rule' – *20th HISWA Symposium on Yacht Design and Construction*, Amsterdam, 2008

[11] Gerhardt F., Flay R., Richards P.: 'Unsteady Aerodynamic Phenomena Associated with Sailing Upwind in Waves', *3rd High performance Yacht Design Conference*, Auckland 2008.

[12] Gerhardt, F. C.; Flay, R.; Richards, P. (2010): Unsteady aerodynamics of two interacting yacht sails in two-dimensional potential flow. *J. Fluid Mech.*, **668**. 551-581

[13] Fossati F., Muggiasca S., 'Sails Aerodynamic Behaviour in Dynamic Conditions', *Proceedings of the 19th Chesapeake Sailing Yacht Symposium*, Annapolis, 2009.

[14] Fossati F., Muggiasca S., 'Experimental Investigation of Sail Aerodynamic Behavior in Dynamic Conditions', *Journal of Sailboat Technology* , 2011-02 SNAME

[15] Viola I., Flay R., 'Pressure distributions on sails investigated using three methods: on water measurements, wind tunnel measurements and CFD', *Proceedings of the 20th Chesapeake Sailing Yacht Symposium*, Annapolis, 2011.

[16] Keuning, J.A., Vermeulen K.J., H.P. ten Have., 'An approximation Method for the added resistance in waves of a sailing yacht', 2nd *International Symposium on Design and Production of Motor and Sailing Yachts MDY '06*, Madrid, Spain, 2006.

[17] Jackson, P.S.: "An improved Upwind Sail Model for VPP's", *Proceedings of the 15th Chesapeake Sailing Yacht Symposium*, Annapolis, 2001.

[18] Augier B., Bot P., Hauville F., Durand M.: 'Experimental validation of unsteady models for wind/sails/ rigging fluid structure interaction', *International Conference on Innovation in High Performance Sailing Yacht*, Lorient, 2010.

[19] Augier B., Bot P., Hauville F.: 'Experimental full scale study on yacht sails and rig under unsteady sailing conditions and comparison to fluid structure interaction unsteady models', *Proceedings of the 20th Chesapeake Sailing Yacht Symposium*, Annapolis, 2011.

[20] Richardt T., Harries S., Hochkirch K., 'Manoeuvring simulations for ships and sailing yachts using FRIENDSHIP Equilibrium as an open modular workbench', *COMPIT*, Hamburg 2005.

[21] Harris D.H., 'Simulation of upwind manoeuvring of a sailing yacht', *Dissertation for Doctor of Philosophy degree,* Univ. of Maryland-College Park, 2002.

[22] Contento G., Ledri M., Codiglia L., 'Experimental Analysis of the Vertical Motions in Waves of an IACC Yacht with Calm Water-Optimized Bulb Shapes', *Proc. of 2nd High Performance Yacht Design Conference, pp.82-88,* Auckland 2006

[23] Gerhardt F., Le Pelley D., Flay R., Richards P.: 'Tacking in the wind tunnel, *19th Chesapeake Sailing Yacht Symposium*, Annapolis, 2009.

[24] Fossati F., Muggiasca S., 'Numerical modeling of sail aerodynamic behaviour in Dynamic Conditions', *International Conference on Innovation in High Performance Sailing Yacht*, Lorient, 2010.

[25] Kerwin, JE "A velocity Prediction Program for Ocean racing yachts", *Rep 78-11 MIT*, July 1978

[26] Le Pelley D., Morris D., Richards P.: 'Aerodynamic force deduction on yacht sails using pressure and shape measurements in real time', *4th High performance Yacht Design Conference*, Auckland 2012.

[27] Fossati F., Muggiasca S.: 'An experimental investigation of unsteady sail aerodynamics including sail flexibility', *4th High performance Yacht Design Conference*, Auckland 2012

[28] Fossati F. **"**Aero-hydrodynamics and the performance of sailing Yachts" *Adlard Coles Nautical*, London 2009

APPENDIX 1

In the following the yacht's velocity and acceleration normal and tangential components given by eqs (5), (6), (7) and (8) will be derived.

Let's consider the vessel on the sea surface at position:

$$\begin{cases} x = x(t) \\ z = f(x(t), t)) \end{cases} \tag{A1}$$

moving with velocity:

$$\begin{cases} V_X = \dfrac{dx(t)}{dt} = \dot{x}(t) \\ V_Z = \dfrac{df(x(t), t))}{dt} = f_x \dot{x} + f_t \end{cases} \tag{A2}$$

Using the free surface angle σ which is defined by:

$$\sigma = tg^{-1}(f_x) \tag{A3}$$

the tangential and normal components of the yacht's velocity V_n and V_t are given by:

$$V_t = V_X \cos\sigma + V_Z \sin\sigma \tag{A4}$$

$$V_n = V_Z \cos\sigma - V_X \sin\sigma \tag{A5}$$

From eq. (A5):

$$\frac{V_n}{\cos\sigma} = V_Z - V_X tg\sigma \tag{A6}$$

But:

$$\left\{ \begin{array}{l} tg\sigma = f_x \\ \cos\sigma = \dfrac{1}{\sqrt{\left(1+tg\sigma_x^2\right)}} = \dfrac{1}{\sqrt{\left(1+f_x^2\right)}} \end{array} \right\} \tag{A7}$$

And substituting in eq. (A6) we obtain:

$$V_n = \left(V_Z - V_X f_x\right)\frac{1}{\sqrt{\left(1+tg\sigma_x^2\right)}} = \left[f_x\dot{x} + f_t - \dot{x}f_x\right]\frac{1}{\sqrt{\left(1+f_x^2\right)}} = f_t\left(1+f_x^2\right)^{-1/2} \tag{A8}$$

that is eq.(5).
Analogously from eq. (A4) we obtain:

$$\frac{V_t}{\cos\sigma} = V_X + V_Z tg\sigma \tag{A9}$$

and substituting eq. (A7) in eq. (A5) we obtain

$$\begin{aligned} V_t &= \left[\dot{x} + \left(f_x\dot{x} + f_t\right)f_x\right]\frac{1}{\sqrt{\left(1+f_x^2\right)}} = \left[\dot{x}\left(1+f_x^2\right) + f_x f_t\right]\left(1+f_x^2\right)^{-1/2} = \\ &= \dot{x}\left(1+f_x^2\right)^{1/2} + f_x f_t \left(1+f_x^2\right)^{-1/2} \end{aligned} \tag{A10}$$

that is eq.(6).

In the same way, considering the yacht's acceleration components:

$$\begin{cases} a_X = \dfrac{dV_X}{dt} = \ddot{x}(t) \\ a_Z = \dfrac{dV_Z}{dt} = f_x \ddot{x} + 2 f_{xt} \dot{x} + f_{xx} \dot{x}^2 + f_{tt} \end{cases} \tag{A11}$$

the tangential and normal components of the yacht's velocity a_n and a_t are given by:

$$a_t = a_X \cos\sigma + a_Z \sin\sigma \tag{A12}$$

$$a_n = a_Z \cos\sigma - a_X \sin\sigma \tag{A13}$$

and taking into account for eq,(A7) substituting eq.(A11) in eq.(A13)

$$\begin{aligned} a_n = a_Z - a_X tg\sigma = a_Z - a_X f_x = \frac{1}{\sqrt{\left(1 + f_x^2\right)}} \left(f_x \ddot{x} + 2 f_{xt} \dot{x} + f_{xx} \dot{x}^2 + f_{tt} - \ddot{x}\ f_x \right) = \\ = \left(1 + f_x^2\right)^{-1/2} \left(f_{xx} \dot{x}^2 + 2 f_{xt} \dot{x} + f_{tt} \right) \end{aligned} \tag{A14}$$

that is eq.(7).

Analogously substituting eq.(A11) in eq.(A12) and taking into account for eq,(A7):

$$\begin{aligned} a_t = \cos\sigma\ \left(a_X + a_Z f_x\right) = \cos\sigma\ \left[\ddot{x} + \left(f_x \ddot{x} + 2 f_{xt} \dot{x} + f_{xx} \dot{x}^2 + f_{tt} \right) f_x \right] = \\ = \left(1 + f_x^2\right)^{-1/2} \left[\ddot{x}\ \left(1 + f_x^2\right) + f_x \left(f_{xx} \dot{x}^2 + 2 f_{xt} \dot{x} + f_{tt} \right)\right] = \\ = \ddot{x}\ \left(1 + f_x^2\right)^{1/2} + f_x \left(1 + f_x^2\right)^{-1/2} \left(f_{xx} \dot{x}^2 + 2 f_{xt} \dot{x} + f_{tt} \right) \end{aligned} \tag{A15}$$

But from eq.(A14) we recognize that:

$$\left(1 + f_x^2\right)^{-1/2} \left(f_{xx} \dot{x}^2 + 2 f_{xt} \dot{x} + f_{tt} \right) = a_n \tag{A16}$$

So from eq.(A16) follows:

$$a_t = \ddot{x} \left(1 + f_x^2\right)^{1/2} + f_x a_n \tag{A17}$$

that is eq.(8).